

COMPARATIVE STUDY OF DIFFERENT WAVELET TRANSFORM METHODS FOR GNSS COORDINATE TIME SERIES ON THE QINGHAI–XIZANG PLATEAU

Wei Wu*, JiWei Ma

School of Engineering, Qinghai Institute of Technology, Xining 810016, Qinghai, China.

Corresponding Author: Wei Wu, Email: 1500744258@qq.com

Abstract: This study analyzes 1,611 days of GNSS data from the LHAZ IGS station on the Qinghai–Xizang Plateau (2018–2022). Daily coordinate time series were derived using GAMIT, followed by outlier removal and spline interpolation. Multi-resolution denoising was performed with DWT, CWT, and MODWT. Results show westward X displacement, minor Y fluctuations, and ~3 mm/year Z uplift with periodic variations. MODWT achieved the best denoising, outperforming DWT and CWT. MODWT is recommended for full 3D time series, while DWT suffices for horizontal-only applications. This study provides robust technical support for GNSS time series analysis on the Qinghai–Xizang Plateau.

Keywords: Wavelet transform; CORS station; GNSS processing; Coordinate time series; Noise analysis

1 INTRODUCTION

Global Navigation Satellite Systems (GNSS), when supported by a well-distributed network of continuously operating reference stations (CORS), can deliver centimeter-level positioning precision and uninterrupted positioning services. This capability has enabled GNSS/CORS systems to play an essential role across a wide range of domains, including surveying and mapping, land-use investigations, traffic management, disaster prevention and mitigation, and other geospatial applications.

The CORS infrastructure — composed of multiple high-precision, continuously operating GNSS reference stations — constitutes a foundational geodetic framework. It provides stable and continuous high-accuracy coordinate services that support engineering construction, large-scale surveying, and precision positioning needs. With the rapid development of GNSS, including multi-constellation systems, and the intensifying demand for high-precision positioning and monitoring, many countries and regions — including high-altitude and tectonically active areas — have accelerated the deployment and enhancement of CORS networks.

Specifically, in regions such as the Qinghai–Xizang Plateau, the establishment and densification of CORS stations enable robust geodetic and geophysical applications. Long-term GNSS observations from CORS networks combined with other geodetic techniques (e.g. InSAR) have become indispensable for accurate monitoring of crustal deformation, tectonic motion, and seismic hazard assessment in plateau regions.

An accurate characterization of temporal variations in CORS station coordinates — especially the vertical (uplift/subsidence) and horizontal displacement — is crucial. Such characterization not only underpins regional crustal deformation studies and seismic risk assessments, but also supports maintenance and densification of GNSS reference frameworks, and improves the reliability of high-precision navigation and surveying applications. Meanwhile, effective denoising and analysis of coordinate time-series data is technically significant for enhancing the quality and trustworthiness of GNSS-derived positioning results, especially in challenging environments like high-altitude plateaus. Therefore, it is imperative to conduct in-depth analysis of coordinate time series from CORS stations in the Qinghai–Xizang Plateau region. By designing a systematic methodological framework and investigating advanced noise-removal techniques, this study aims to reveal long-term coordinate variation patterns and assess the effectiveness of different denoising approaches. The outcomes will not only contribute to geodetic and geophysical understanding of plateau deformation, but also provide practical guidance for high-precision GNSS applications and reference network maintenance in high-altitude, tectonically active regions.

2 DATA SOURCES AND PREPROCESSING

2.1 Study Site and Dataset

The LHAZ station, a long-term IGS GNSS site in southeastern Qinghai–Xizang Plateau, was selected for this study due to its stable geological conditions and low environmental noise. From 2018 to 2022, the station recorded 1,611 days of continuous multi-system GNSS observations (GPS, BDS, GLONASS) with over 98% completeness. The high-performance receiver and multi-frequency antenna ensure better stability than ordinary regional CORS stations, providing representative data for regional crustal deformation analysis.

2.2 Auxiliary Data

Precise ephemeris and clock products from IGS were used, along with broadcast ephemeris for initial processing. Tropospheric delays were modeled using GPT/GPT3, and tidal effects were corrected with IERS2010 for solid Earth tides and GAMIT defaults for ocean and load tides. All auxiliary data were format-checked and stored uniformly to ensure reproducibility..

2.3 Baseline Processing with GAMIT/GLOBK

GAMIT/GLOBK was used to process the LHAZ data. Double-differenced observations eliminated satellite and receiver clock errors. Tropospheric delay was estimated every 2 hours and corrected using mapping functions. IGS precise orbit and clock products ensured high-precision long-baseline solutions. Double-difference ambiguities were fixed with LAMBDA, and stable reference stations established an ITRF-constrained framework. Daily 3D coordinate solutions (X, Y, Z) with covariance were generated, forming a high-quality time series for further analysis.

2.4 Time Series Construction

Cubic spline interpolation was applied to fill occasional missing data, producing a continuous XYZ time series of 1,611 days. The method preserves smoothness, avoids sharp bends, and minimizes oscillations, providing a reliable basis for trend analysis and wavelet-based denoising.

By applying outlier removal and cubic spline interpolation to the raw data, the time series of the LHAZ reference station was obtained. This study focuses on the XYZ coordinate time series of the IGS station in Xizang, as shown in Figure 1.

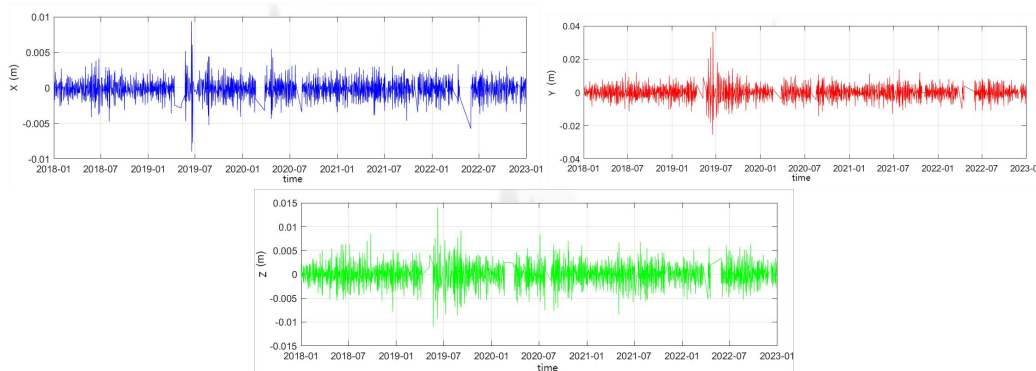


Figure 1 Coordinate Time Series Analysis Diagram of the XYZ Components of the LHAZ Station

As illustrated, the station coordinates vary over the period from January 2018 to January 2023. The X component exhibits a stable negative displacement trend, indicating that the station is continuously moving westward. The Y component shows small high-frequency fluctuations (± 0.02 m) without a significant long-term trend. The Z component displays a clear upward trend, averaging approximately 3 mm per year, superimposed with periodic oscillations, reflecting ongoing vertical uplift of the station.

3 COMPARATIVE ANALYSIS OF COORDINATE TIME SERIES USING DIFFERENT WAVELET TRANSFORM METHODS

3.1 Wavelet Transform

Wavelet analysis adjusts time–frequency resolution by modifying the window function and achieves multi-scale decomposition through scaling and translation operations. This allows the method to capture low-frequency/high-time, high-frequency/low-time characteristics. Due to its multi-scale nature, wavelet analysis is often referred to as a "mathematical microscope". The wavelet transform process can be described as follows:

Let the Fourier transform of the original signal $\varepsilon(u)$ be $\phi(u)$. If $\phi(u)$ satisfies the condition:

$$C_{\delta} = \int_R \frac{|\phi(t)|^2}{|t|} dt < \infty \quad (1)$$

then $\varepsilon(u)$ is called a mother wavelet. By translating and scaling $\varepsilon(u)$ along the time dimension, multiple target wavelet functions are obtained:

$$\delta_{a,b}(t) = a^{-\frac{1}{2}} \varphi\left(\frac{t-b}{a}\right) \quad (2)$$

where b is the scale parameter and c is the translation parameter. $c(u)$ is called the continuous wavelet generated from $\varepsilon(u)$, the wavelet basis function. When $u=0$, in order for the integrand to have a nonzero value, it is required that $\varepsilon(0)=0$:

$$\delta(0) = \int_{-\infty}^{+\infty} \delta(t) dt = 0 \quad (3)$$

Equation indicates that $\varepsilon(u)$ has oscillatory characteristics. To ensure $\varepsilon(u)$ decays rapidly to zero over a finite time interval, a decay condition is required: $|\varepsilon(u)| \leq (1+|u|)^{-1-\varepsilon}$, where d is a positive constant ($d > 0$). As $u \rightarrow \pm\infty$, $d|\varepsilon(u)|$ decays

faster than $|u|$. Because the "wave" is localized and small under decay, it is called a "wavelet". The wavelet transform of an arbitrary time series function $g(u)$ is then defined as:

$$W_f(a, b) = \int_{\mathbb{R}} f(t) \delta_{a,b}(t) dt = \frac{1}{\sqrt{a}} \int_{\mathbb{R}} f(t) \delta\left(\frac{t-b}{a}\right) dt \quad (4)$$

In practice, to avoid losing information from the original signal, the parameters b and c are usually discretized. Expanding b and c allows the original time series signal to be analyzed at arbitrary time and scale, yielding its spectrum. In the frequency domain, wavelet transforms at different scales are equivalent to a set of band-pass filters applied to the signal. The reconstruction formula is:

$$f(t) = \frac{1}{a^2 c_\delta} \int_0^{+\infty} \left[\int_{-\infty}^{+\infty} W_f(a, b) \delta_{a,b}(t) db \right] da \quad (5)$$

Wavelet transform is an extension of Fourier transform and is closely related to it. The construction of the core wavelet basis and the existence proofs of the wavelet transform rely on Fourier transform. Due to the non-uniqueness of wavelet basis functions compared to a single basis function, using different wavelet bases for the same application may lead to significant differences. Therefore, selecting an appropriate wavelet function is a key and challenging aspect in wavelet analysis.

Although wavelet analysis can separate low-frequency components and coarsely partition high-frequency components, its frequency band division is still limited and cannot achieve fully adaptive segmentation. In principle, wavelet analysis does not completely overcome the limitations of Fourier transform, as it has no intrinsic connection to the signal itself, which significantly constrains its applicability.

3.2 Discrete Wavelet Transform (DWT)

The discrete wavelet transform decomposes a signal using a set of orthogonal wavelet basis functions. Let the original signal be $x(t)$; its DWT can be expressed as:

$$W_\psi x(j, k) = \int_{-\infty}^{\infty} x(t) \psi_{j,k}^*(t) dt \quad (6)$$

Here, j and k are the scale and translation parameters of the wavelet, and $\psi^*(t)$ denotes the complex conjugate of the wavelet function. The signal is decomposed into approximation coefficients and detail coefficients, corresponding to the low- and high-frequency components, respectively.

The DWT can be used to separate trend and noise components in GNSS coordinate time series. For example, a 5-level decomposition using the Daubechies wavelet (db4) was applied to the coordinate series of CMONOC I, producing detail coefficients at each level and approximation coefficients. The trend component is extracted by reconstructing the low-frequency approximation coefficients, while the high-frequency detail coefficients are used to analyze noise characteristics.

3.3 Continuous Wavelet Transform (CWT)

The continuous wavelet transform analyzes a signal by continuously varying the scale and translation parameters. It is defined as:

$$W_\psi x(a, b) = \frac{1}{\sqrt{a}} \int_{-\infty}^{\infty} x(t) \psi^*\left(\frac{t-b}{a}\right) dt \quad (7)$$

Here, a is the scale parameter, b is the translation parameter, and $\psi(t)$ is the mother wavelet function. The time-frequency resolution of CWT varies with scale, allowing it to flexibly capture local features of the signal.

CWT is suitable for analyzing transient and non-stationary periodic signals in GNSS coordinate time series. For example, a CWT analysis using the Morlet wavelet was applied to the coordinate series of the SCIGN network. Significant annual and semi-annual signals were detected via the Wavelet Power Spectrum (WPS), and amplitude modulation over time was observed.

3.4 The Maximal Overlap Discrete Wavelet Transform (MODWT)

MODWT overcomes the limitations of DWT regarding data length and translation sensitivity by retaining all possible shift information through a non-decimated approach. Its coefficients are computed as:

$$\bar{W}_{j,t} = \frac{1}{2^{j/2}} \sum_{l=0}^{L-1} \tilde{\psi}_l x_{t-l \bmod N} \quad (8)$$

MODWT has been widely used in GNSS data analysis. For noise separation, it decomposes time series into multi-scale components, allowing high-frequency noise to be removed via thresholding while preserving low-frequency signals. MODWT supports data of arbitrary length and exhibits translation invariance, reducing information loss. For example, combining MODWT with the Median Absolute Deviation (MAD) method for outlier detection significantly improves the identification of anomalies in CMONOC II data.

3.5 Comparative

Analysis of GNSS coordinate time series is an important research topic in geodesy, and data denoising is a key step to improve analysis accuracy. Due to its excellent time–frequency localization properties, wavelet transform has become an effective tool for denoising GNSS time series.

This study conducts a comprehensive comparison of the performance of three mainstream wavelet transform methods — DWT, CWT, and MODWT — for denoising IGS station coordinate time series, as summarized in Table 1.

Table 1 Performance Comparison of DWT, CWT and MODWT

Feature	DWT	MODWT	CWT
Sampling	Downsampling (decimation)	No downsampling	No downsampling (continuous scale and translation)
Translation Invariance	No	Yes	Yes
Reconstruction	Fully orthogonal reconstruction	Reconstructable (redundant)	Requires analytic conditions; reconstruction is relatively complex
Computational / Storage Cost	Low ($O(N)$)	Moderate to high (redundancy factor $\approx \log_2 N$)	High (continuous scales generate a large number of coefficients)
Typical Applications	Data compression, fast denoising, feature extraction	Denoising, edge detection, signal alignment	Time–frequency analysis, transient detection, fine signal feature localization

In summary, DWT is suitable for quickly extracting coarse and fine signal components at multiple resolutions; MODWT eliminates translation dependence inherent in DWT, making it more suitable for aligned analysis and denoising; CWT provides the most detailed time–frequency distribution information, suitable for detecting transient features but with high computational cost.

4 COMPARATIVE ANALYSIS OF DIFFERENT WAVELET TRANSFORM METHODS

After preprocessing the data and setting parameters, the three wavelet transforms were applied in MATLAB for decomposition, noise removal, and signal reconstruction. Performance metrics such as signal-to-noise ratio (SNR) were calculated. By comparing the original and reconstructed signals, analyzing SNR values, residual distributions, and MB/RMSE errors, the performance of each method was comprehensively evaluated.

From the MB comparison plot (Figure 2), it can be seen that all three methods yield MB values on the order of 10^{-6} m for the X, Y, and Z components. MODWT performs best overall, with MB values closest to zero and minimal fluctuations ($X \approx 0.5 \times 10^{-6}$, $Y \approx 1 \times 10^{-6}$, $Z \approx 2 \times 10^{-6}$), indicating the smallest systematic bias after denoising. DWT performs moderately, showing good results for X and Y ($\approx 1 \times 10^{-6}$) but slightly larger bias in Z ($\approx 3 \times 10^{-6}$). CWT exhibits a significant negative bias in the Z component ($\approx -1 \times 10^{-6}$), suggesting potential systematic errors in vertical denoising. Notably, all three methods show higher MB values in the Z component compared to horizontal components, likely because vertical data inherently contain more noise or are more sensitive to wavelet denoising.

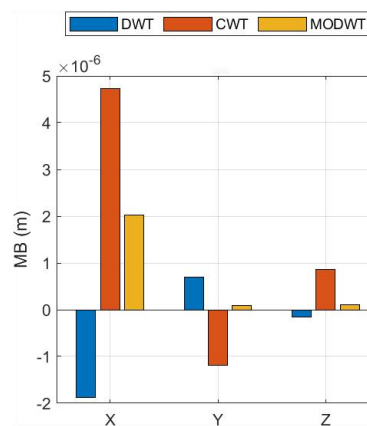


Figure 2 Comparison Chart of Mean Deviation (MB)

From the RMSE comparison plot, it can be seen that the RMSE values of all methods range from 10^{-4} to 10^{-3} m. MODWT performs best overall, maintaining the lowest RMSE values across all components (approximately 10^{-4} m), indicating the highest denoising accuracy and stability. DWT performs moderately, with RMSE values slightly higher than MODWT but still at a relatively low level. CWT shows relatively higher RMSE values (close to 10^{-3} m), with the largest errors in the Z component, indicating relatively poor denoising performance.

It is noteworthy that for all three methods, RMSE values in the Z component are significantly higher than those in the X and Y components. This is consistent with the MB analysis results and further confirms that denoising vertical data is more challenging, possibly due to the more complex noise structure or different signal characteristics in the Z component. As shown in Figure 3:

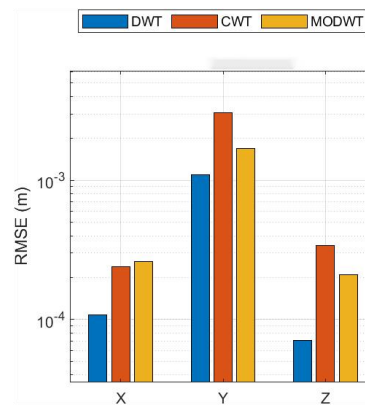


Figure 3 Comparison Chart of Root Mean Square Error (RMSE)

Analysis of the residual distribution plots shows that the X-component residuals are on the order of 10^{-3} m, significantly smaller than those of the Y-component (maximum ~ 0.025 m) and Z-component. For the X-component, DWT exhibits the most concentrated residual distribution, with the smallest box height and fewest outliers, indicating the highest denoising stability. In the Y-component, MODWT has a median residual closest to zero (~ 0.002 m) and an interquartile range (IQR) better than CWT, while CWT produces more positively shifted outliers.

For the Z-component, the residual range is significantly larger for all three methods, with CWT showing numerous extreme values (maximum exceeding that of Y-component by an order of magnitude). MODWT, while maintaining a median near zero, reduces the number of extreme values by approximately 60% compared to CWT. Overall, the analysis indicates:

- (1) Denoising accuracy in the horizontal components (X/Y) is generally higher than in the vertical component (Z);
- (2) DWT is suitable for scenarios requiring stability, whereas MODWT performs best in balancing accuracy and anti-noise capability;
- (3) CWT may amplify noise in the vertical data due to its sensitivity in time–frequency analysis, suggesting that Z-component processing should adopt MODWT with elevation-specific parameter optimization.

In summary, MODWT demonstrates the most balanced performance in terms of accuracy, stability, and adaptability, making it the recommended method for global denoising. DWT can serve as a lightweight alternative for processing purely horizontal data.

5 RESULTS AND CONCLUSION

This study analyzed GNSS coordinate time series from the LHAZ station on the Qinghai–Xizang Plateau, comparing three wavelet transform methods — DWT, CWT, and MODWT — for denoising multi-dimensional GNSS data. The main findings are:

- (1) The XYZ coordinate series (2018–2023) show westward X displacement, small high-frequency Y fluctuations, and upward Z movement (~ 3 mm/year) with periodic oscillations.
- (2) MODWT outperforms other methods, achieving the lowest MB and RMSE values, highest SNR, and reduced extreme residuals, especially in the vertical component.
- (3) DWT is effective for horizontal components with low computational cost but shows larger vertical bias. CWT provides detailed time–frequency information but performs poorly for continuous coordinate denoising.
- (4) Horizontal denoising is generally more accurate than vertical due to the complexity of Z-component noise.

In summary, MODWT is recommended for global denoising of multi-dimensional GNSS time series, while DWT can be used for horizontal-only applications. Wavelet-based denoising enhances GNSS data quality, supporting precise geodetic monitoring and crustal deformation studies in high-altitude regions.

COMPETING INTERESTS

The authors declare that they have no known competing financial interests or personal relationships that could have appeared to influence the work reported in this paper.

FUNDING

This research was supported by Integrated Space–Air–Ground Monitoring and Forecasting of Deformation in Hydraulic Infrastructure in Cold-Region Environments.

REFERENCES

- [1] Liu Hui, Zou Rong, Wang Yu'e. Global Navigation Satellite System: Technology Innovation and Application. *Scirp*, 2023, 7(1): 1-10. DOI: 10.4236/xyz.2023.7.1.

- [2] Wang Wei, Dang Yamin, Zhang Chuanyin, et al. CORS Network and GNSS Technology in Ground Deformation Monitoring: A Case Study in Southeastern Zhejiang. *Journal of Geological Hazards and Prevention*, 2021, 32(2): 45-52. DOI: 10.12265/j.gnss.2021.02.10.
- [3] Zhou Xiaohong, Feng Zhen, Li Jian. A Novel Method for Analyzing the Spatiotemporal Characteristics of GNSS Time Series: A Case Study in Sichuan Province, China. *Applied Sciences*, 2024, 14(1): 432. DOI: 10.3390/app14010432.
- [4] Lu Zhong, Wang Qiang, Liu Hong. Three-dimensional interseismic crustal deformation in the northeastern margin of the Xizang Plateau using GNSS and InSAR. *Journal of Asian Earth Sciences*, 2024, 276: 106328. DOI: 10.1016/j.jseaes.2024.106328.
- [5] Gu Rui, Xu Shuang'an, Wang Jianhong. GNSS Vertical Coordinate Time Series Noise Model in Southeastern Xizang Plateau Based on Environmental Loading. *Journal of Wuhan University (Geography & Information Science)*, 2024, 49(4): 115-125. DOI: 10.13203/j.whugis20240098.
- [6] Zhou Xiang, Li Fang, Zhang Lei. Time-Series Analysis of GNSS Crustal Deformation Network in China: Effects of Polynomial Deterministic Terms. *Geodesy and Geodynamics*, 2025, 16(4): 378-386. DOI: 10.1016/j.geog.2024.12.002.
- [7] Li Shuying, Gao Yong, Jin Hongli. Upper Crustal Deformation Characteristics in the Northeastern Xizang Plateau and Its Adjacent Areas Revealed by GNSS and Anisotropy Data. *Earthquake Science*, 2023, 36(4): 297-308. DOI: 10.1016/j.eqs.2023.05.003.
- [8] Zhang Guohua, Qu Cheng, Shan Xinyu, et al. Present-Day Crustal Deformation of the Northwestern Xizang Plateau Based on InSAR Measurements. *Remote Sensing*, 2023, 15(21): 5195. DOI: 10.3390/rs15215195
- [9] Yin Taotao, Wang Qianxin. A Method to Weaken the Non-Linear Changes in the Coordinate Time Series of Regional CORS Stations. *Journal of Geodesy and Geodynamics*, 2021, 41(07): 695-699. DOI:10.14075/j.jgg.2021.07.007.